THE EMDRIVE – A NEW SATELLITE PROPULSION TECHNOLOGY

Roger Shawyer C.Eng. MIET. FRAeS
SPR Ltd, United Kingdom

Biography

Roger Shawyer is a Director of Satellite Propulsion Research Ltd (SPR). Early career experience in the Defence Industry, included R&D work on guided missiles, radars, and communication systems. This was followed by 20 years in the Space industry at EADS Astrium, which included appointments as Head of Department for payload equipment, and as Project Manager for a number of large communications payloads. Responsibilities also covered the initial design of the Galileo navigation payload and signal structure. SPR was set up in 2001, and has carried out a continuous R&D programme in EmDrive technology using UK government funding, private investment and industry contracts.

1. INTRODUCTION

EmDrive technology provides direct conversion of electrical energy to thrust, using radiation pressure at microwave frequencies in a tapered, high Q, resonant cavity. For the first time, propulsion without the need for expelling reaction mass has been demonstrated. As the theory and experimental work clearly shows however, EmDrive is not a reactionless machine. It obeys Newtonian physics by producing an accelerating, reaction force opposite to the thrust vector. The law of conservation of energy is also obeyed, as is well illustrated by applying the dynamic thrust equation to a very high Q, superconducting thruster.

The paper gives a summary of the theory behind EmDrive, followed by answers to the most frequently asked questions concerning the production of net force, conservation of momentum and conservation of energy. The theory clearly derives equations for both static and dynamic thrust.

Under the SPR programme, non linear cavity design software has been developed. This was verified during the manufacture and test of four different thrusters. The test programmes have consistently and repeatedly given thrust and acceleration measurements in close agreement with theoretical predictions. Great emphasis has been placed on eliminating or calibrating out any spurious force data during the tests, and technical reports have been independently reviewed by government and industry experts.

EmDrive technology is now under development in China and the USA. The North Western Polytechnical University in Xian took the basic theory from the SPR website, and developed their own theoretical model. Based on this, they have manufactured and successfully tested an S Band Thruster. The work was then reproduced at a government research institute in Beijing. Development work is now continuing on a 3kW Thruster.

The technology has also been transferred to the USA, under a Technology Assistance Agreement (TAA) sanctioned by the US State Department, and an export licence granted by the UK government. Boeing are currently developing an experimental thruster. EmDrive has also been studied by DARPA and has been the subject of R&D solicitations to the US space industry.

2. PRINCIPLE OF OPERATION

The concept of the microwave engine is illustrated in fig 1. Microwave energy is fed from a magnetron, via a tuned feed to a closed, tapered waveguide, whose overall electrical length gives resonance at the operating frequency of the magnetron.

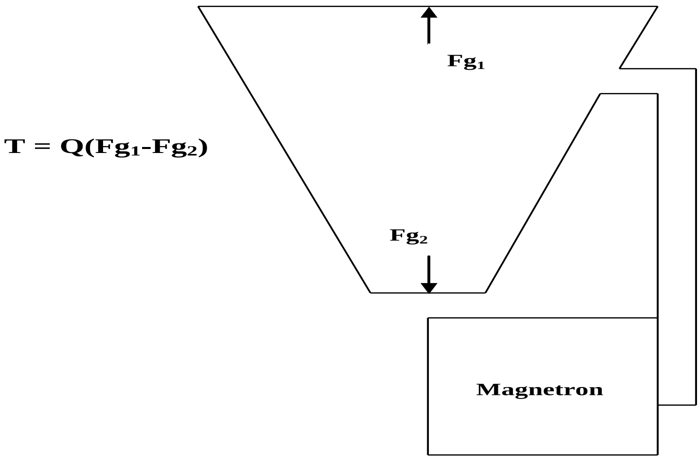

Fig 1

The group velocity of the electromagnetic wave at the end plate of the larger section is higher than the group velocity at the end plate of the smaller section. Thus the radiation pressure at the larger end plate is higher that that at the smaller end plate. The resulting force difference (F_{g1} -F_{g2}) is multiplied by the Q of the resonant assembly.

This force difference is supported by inspection of the classical Lorentz force equation

$$F = q(E + vB) \qquad (1)$$

If v is replaced with the group velocity v_g of the electromagnetic wave, then equation 1 illustrates that if v_{g1} is greater than v_{g2}, then F_{g1} should be expected to be greater than $F_{g2.}$

However as the velocities at each end of the waveguide are significant fractions of the speed of light, a derivation of the force difference equation invokes the difference in velocities and therefore must take account of the special theory of relativity.

Relativity theory implies that the electromagnetic wave and the waveguide assembly form an open system. Thus the force difference results in a thrust which acts on the waveguide assembly.

3. DERIVATION OF BASIC THRUST EQUATION

Consider a beam of photons incident upon a flat plate perpendicular to the beam. Let the beam have a cross-sectional area *A* and suppose that it consists of *n* photons per unit volume. Each photon has energy *hf* and travels with velocity *c*, where *h* is Planck's constant and *f* is the frequency. The power in the incident beam is then

$$P_0 = nhfAc \qquad (2)$$

The momentum of each photon is *hf/c* so that the rate of change of momentum of the beam at the plate (assuming total reflection) is *2nhfA*. Equating this change of momentum to the force F_0 exerted on the plate, we find

$$F_0 = 2nhfA = \frac{2P_0}{c} \qquad (3)$$

(3)

which is the classical result for the radiation pressure obtained by Maxwell (reference 1). The derivation given here is based on Cullen (reference 2). If the velocity of the beam is *v* then the rate of change of momentum at the plate is *2nhfA(v/c)*, so that the force F_g on the plate is in this case given by

$$F_g = \frac{2P_0}{c}(v/c) \qquad (4)$$

We now suppose that the beam enters a vacuum-filled waveguide. The waveguide tapers from free-space propagation, with wavelength λ_0, to dimensions that give a waveguide wavelength of λ_g and propagation velocity v_g. This is the group velocity and is given by

$$v_g = \frac{c}{\sqrt{\mu_r e_r}}\frac{\lambda_0}{\lambda_g} \qquad (5)$$

Then from (4) and (5) (with $\mu_r = e_r = 1$) the force on the plate closing the end of the waveguide is

$$F_g = \frac{2P_0}{c}(v_g/c) = \frac{2P_0}{c}\frac{\lambda_0}{\lambda_g} \qquad (6)$$

see Cullen (p.102 Eq. (15).

Assume that the beam is propagated in a vacuum-filled tapered waveguide with reflecting plates at each end. Let the guide wavelength at the end of the largest cross-section be λ_{g1} and that at the smallest cross-section be λ_{g2}. Then application of (6) to each plate yields the forces

$$F_{g1} = \frac{2P_0}{c}\frac{\lambda_0}{\lambda_{g1}} \qquad\qquad F_{g2} = \frac{2P_0}{c}\frac{\lambda_0}{\lambda_{g2}}$$

Now $\lambda_{g2} > \lambda_{g1}$, due to the difference in cross-section, and hence $F_{g1} > F_{g2}$.
Therefore the resultant thrust T will be

$$T = F_{g1} - F_{g2} = \frac{2P_0}{c}\left(\frac{\lambda_0}{\lambda_{g1}} - \frac{\lambda_0}{\lambda_{g2}}\right) \qquad (7)$$

4. FREQENTLY ASKED QUESTIONS

Four questions have been identified which cause most of the difficulties in understanding the concept.

(a) How can net thrust be produced ?

From (7) it can be seen that to maximise thrust, the taper design should ensure λ_{g1} approaches λ_0 consistent with an acceptable maximum dimension. Also λ_{g2} should approach infinity, which occurs when the minimum dimension approaches the propagation cut-off limit. This minimum dimension must be consistent with allowable manufacturing and thermal tolerances.

The resulting design must also ensure a low taper slope, to minimise the axial component of side wall forces. This combination of dimensional constraints requires an iterative numerical design approach, taking account of the highly non-linear relationship between radial dimensions and guide wavelengths. This relationship is illustrated in fig 2.

Fig 2 Guide wavelength for circular TMO1 at 2 GHz

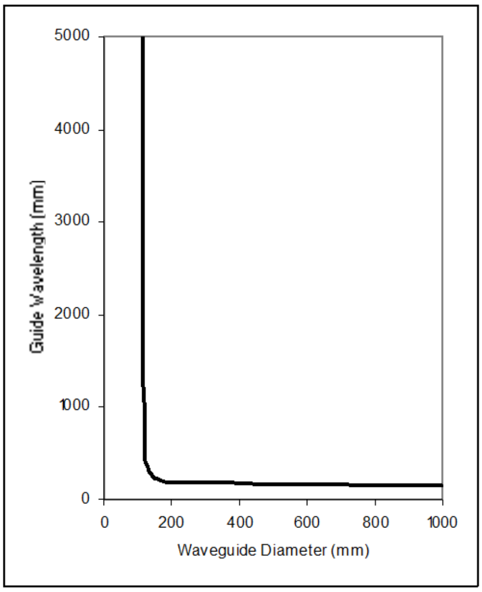

It is clear that if the minimum dimension was the cut off diameter, force F_{g2} would be zero. However because there would still be a significant small end plate area, the projected area of the side wall would not equal the area of the large end plate. Thus any attempt to show a resultant zero net force due to equalisation of areas is incorrect.

Note also that if the forces had been the mechanical result of a working fluid within the closed waveguide assembly, then the resultant force would merely introduce a mechanical strain in the waveguide walls. This would be the result of a closed system of waveguide and working fluid.

In the present system, the working fluid is replaced by an electromagnetic wave propagating close to the speed of light and Newtonian mechanics must be replaced with the special theory of relativity. There are two effects to be considered in the application of the special theory of relativity to the waveguide. The first effect is that as the two forces F_{g1} and F_{g2} are dependent upon the velocities v_{g1} and v_{g2}, the thrust T should be calculated according to Einstein's law of addition of velocities given by

$$v = \frac{v_1 + v_2}{1 + (v_1 v_2)/c^2}$$

The second effect is that as the beam velocities are not directly dependent on any velocity of the waveguide, the beam and waveguide form an open system. Thus the reactions at the end plates are not constrained within a closed system of waveguide and beam, but are reactions between waveguide and beam, each operating within its own reference frame, in an open system.

From (7) and (5) we find

$$T = \frac{2P_0}{c}\left(\frac{v_{g1}}{c} - \frac{v_{g2}}{c}\right)$$

where

$$v_{g1} = c\lambda_0 / \lambda_{g1} \quad v_{g2} = c\lambda_0 / \lambda_{g2}.$$

Applying the above addition law of relativistic velocities we obtain

$$T = \frac{2P_0}{c^2}\left(\frac{v_{g1} - v_{g2}}{1 - v_{g1}v_{g2}/c^2}\right) = \frac{2P_0 S_0}{c}\left(\frac{\lambda_0}{\lambda_{g1}} - \frac{\lambda_0}{\lambda_{g2}}\right)$$

(8)

where the correction factor S_o is

$$S_0 = \left\{1 - \frac{\lambda_0^2}{\lambda_{g1}\lambda_{g2}}\right\}^{-1}$$

We suppose that the waveguide is resonant at the frequency of the microwave beam and that the conductive and dielectric losses are such that there are Q return paths (each at power P_0). Then the total thrust is finally given by

$$T = \frac{2P_0 Q S_0}{c}\left(\frac{\lambda_0}{\lambda_{g1}} - \frac{\lambda_0}{\lambda_{g2}}\right) \qquad (9)$$

(b) How is momentum conserved?

The concept of the beam and waveguide as an open system can be illustrated by increasing the velocity of the waveguide in the direction of the thrust, until a significant fraction of the speed of light is reached. Let v_w be the velocity of the waveguide. Then as each plate is moving with velocity v_w the forces on the plates, given by equation 6, are modified as follows:

$$F_{g1} = \frac{2P_0}{c^2}\left(\frac{v_{g1} - v_w}{1 - v_{g1}\, v_w / c^2}\right) = \frac{2P_0}{c^2} v_{ga}$$

and

$$F_{g2} = \frac{2P_0}{c^2}\left(\frac{v_{g2} + v_w}{1 + v_{g2}\, v_w / c^2}\right) = \frac{2P_0}{c^2} v_{gb}$$

The thrust is then given by

$$T = \frac{2P_0}{c^2}\left(\frac{v_{ga} - v_{gb}}{1 - v_{ga}\, v_{gb} / c^2}\right) \qquad (10)$$

The solution to (10) is illustrated in Fig 3. Note that to maintain the principle of the conservation of momentum, the acceleration of the waveguide due to thrust, is opposite to the actual thrust direction. Thus, in Fig 3, the sign convention for the waveguide velocity axis is:

Acceleration Vector Thrust Vector

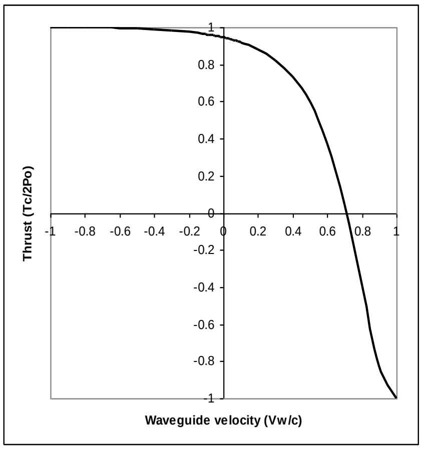

Fig 3. Solution to equation 10

When the waveguide is accelerated along the acceleration vector, the thrust approaches a maximum of 1. However, as the velocity of the waveguide increases in the direction of thrust, the thrust will decrease to zero. This point is reached when $v_{ga} = v_{gb}$. Fig 3 illustrates the solution to equation 10 for values of $v_{g1} = 0.95\,c$ and $v_{g2} = 0.05c$. It can be seen that if v_w is increased beyond the value of $0.7118c$, the thrust reverses.

Equation 10 illustrates that the thruster is an open system, where guide velocities are independent of waveguide velocity, and it is the relative velocities that give rise to the forces. Note that if Einstein's law for the addition of velocities had not been used, relative velocities would exceed c, and the thrust would go above the theoretical limit of 1.

(c) How is energy conserved?

We now examine the implications of the principle of the conservation of energy when the thrust is first measured on a static test rig, and then when an engine is used to accelerate a spacecraft.

With the microwave engine mounted on a static test rig, all the input power P_0 is converted to electrical loss. In this case the Q of the engine may be termed Q_u, the unloaded Q.

Now $$Q_u = \frac{P_c}{P_0} = \frac{P_c}{P_e}$$

where P_c is the circulating power within the resonant waveguide and P_e is the electrical loss. From (9) we find

$$T = \frac{2P_0 D_f Q_u}{c},$$

Where D_f is the design factor

$$D_f = S_0\left(\frac{\lambda_0}{\lambda_{g1}} - \frac{\lambda_0}{\lambda_{g2}}\right)$$

Then $$T = \frac{2D_f P_c}{c}. \qquad (11)$$

Thus if the circulating power remains constant, for instance in a superconducting resonant waveguide, then T will remain constant. This will be important in non spacecraft applications where very high values of Q_u could be employed to provide a constant thrust to counter gravitational force.

If the engine is mounted in a spacecraft of total mass M and is allowed to accelerate from an initial velocity v_i to a final velocity v_f in time Δt, then by equating kinetic energies we obtain:

$$P_k \Delta t = \frac{M}{2}\left(v_f^{\,2} - v_i^{\,2}\right)$$

where P_k is the output power transferred to the spacecraft. From this we obtain

$$P_k \Delta t = \frac{M}{2}\left(v_f - v_i\right)\left(v_f + v_i\right),$$

so that $$P_k = M\bar{v}a \qquad (12)$$

where $\bar{v}$ is the average velocity over time Δt and a is the acceleration of the spacecraft.
Now $M.a$ is the force due to the acceleration of the spacecraft, which opposes the thrust of the engine. Then

$$P_k = \frac{2P_0 Q_l D_f \bar{v}}{c} \qquad (13)$$

where Q_l is the loaded Q of the engine when it is delivering an output power P_k.

The electrical power losses P_e are assumed to be I^2R losses and thus for any value of Q ,

$$P_e = Q^2 P_{e0}$$

where P_{e0} is the loss for $Q=1$. From the static case, we have

$$P_{e0} = \frac{P_0}{{Q_u}^2}$$

so that

$$P_e = P_0 \left(\frac{Q_l}{Q_u} \right)^2 \qquad (14)$$

For an accelerating spacecraft,

$$P_0 = P_e + P_k$$

Substitution of (13) and (14) into this last equation then yields

$$\left(\frac{Q_l}{Q_u} \right)^2 + \frac{2 Q_l D_f \bar{v}}{c} = 1 \qquad (15)$$

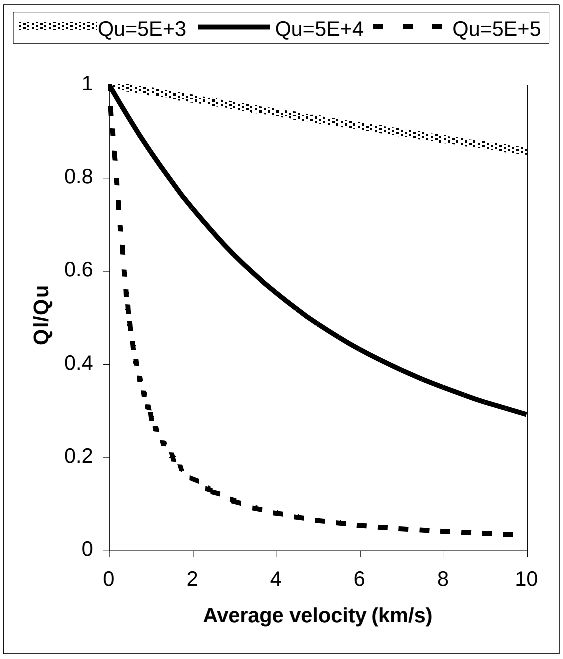

Fig 4 Solution to equation 15.

Fig 4 shows the solution to (15) for values of $\bar{v}$ up to 10km/sec and for values of Q_u equal to $5x10^3$, $5x10^4$ and $5x10^5$. The value of D_f is taken to be 0.945.

For D_f equal to 0.945 and an average velocity of 3 km/s, the specific thrust is obtained from (9) and (15) and is given in fig 5. This illustrates that the specific thrust increases to a maximum of 333 mN/kW at this velocity.

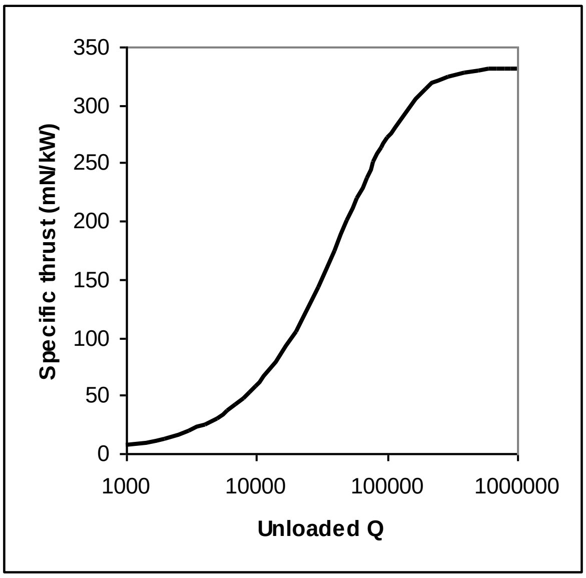

Fig 5 Specific thrust at 3km/s.

(d) Is EmDrive similar to anything else?

EmDrive is a new class of electrical machine operating at microwave frequencies, and therefore bears little similarity to any other device. However, analogies are sometimes helpful in obtaining a mental picture of operating principles and the following mechanical analogy is offered for consideration.

EmDrive can be considered as an "electromagnetic flywheel". As with a mechanical flywheel, a resonant cavity can store energy in the form of momentum. Due to the asymmetric geometry of the EmDrive cavity, the stored momentum can produce a linear force, which if used to accelerate a mass, transfers some of the momentum from the cavity. This transfer results in a loss of Q, and hence a reduction in the force available. However unlike a mechanical flywheel, the cavity is able to store and replace momentum very rapidly. The time constant of, a simple cavity operating at 4 GHz with a Q of 50,000 is 2 microseconds. Thus if acceleration is restricted, as with a large spacecraft being propelled with low thrust, continuous momentum transfer can take place, whilst maintaining the high Q.

5. EXPERIMENTAL PROGRAMME

The first experimental thruster was a 160 mm diameter device, operating at 2.45 GHz. The design factor, calculated from as-built measurements of the thruster geometry was 0.497. In 2001 a test programme was started and an unloaded Q of 5,900 was measured. The maximum thrust, measured using a precision balance was 16mN for an input power of 850W, which is very close to the thrust of 16.6mN predicted from equation (9).

The thrust could be varied from zero to maximum by varying the input power, or by varying the resonant frequency of the thruster. Considerable efforts were made to test for possible thermal and electromagnetic spurious effects. The primary method was to carry out all tests in both nominal and inverted orientations, and to take the mean of the results. The thruster was also sealed into a hermetic enclosure to eliminate buoyancy effects of the cooling air. Three different types of test rig were used, two using 1 mg resolution balances in a counterbalance test rig and one using a 100 mg resolution balance in a direct measurement of thruster weight.

Comparison of the rates of increase of thrust for the different spring constants, using pulsed input power, gave a clear proof that the thrust was produced by momentum transfer and was not due to any "undefined" spurious effect. The total test programme encompassed 450 test runs of periods up to 50 seconds, using 5 different magnetrons.

In 2003 a Demonstrator Engine development programme was started. Unlike the first experimental thruster, the Demonstrator Engine was rated for continuous operation and extensive design work was required to increase the specific thrust by raising the design factor and unloaded Q.

The engine was built to operate at 2.45 GHz, with a design factor of 0.844 and has a measured maximum Q of 45,000 for an overall diameter of 280 mm. The microwave source is a water cooled magnetron with a variable output power up to a maximum of 1.2 kW.

To obtain the predicted thrust, the engine was required to maintain stable resonance at this high Q value. Major design challenges included thermal compensation, tuning control and source matching.

The engine was tested in a large static test rig employing a calibrated composite balance to measure thrust in both vertical and horizontal directions. A total of 134 test runs were carried out over the full performance envelope.

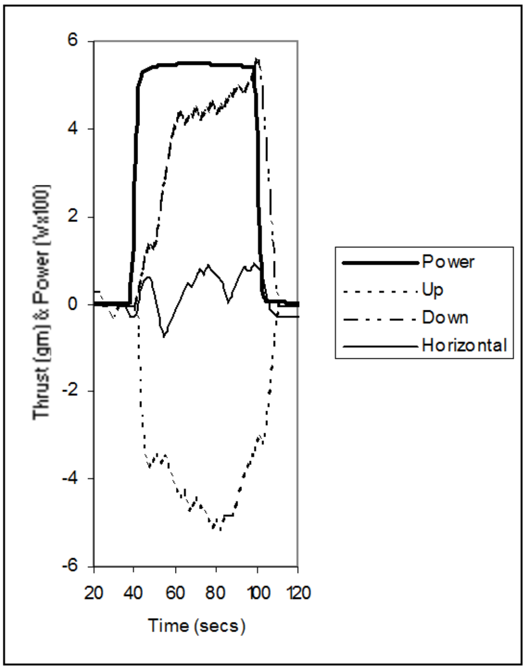

Fig 7. Demonstrator Engine Static Test Data

Fig 7 gives test results for 3 Vertical Thrust test runs under the same input and tuner conditions but for thrust vectors in the Up, Down and Horizontal directions. This clearly illustrates the loss of measured weight for the Up vector, the increase in measured weight for the Down vector, and a mean weight change close to zero, for the horizontal vector. These early, low Q, comparative tests yielded specific thrusts around 80mN/kW.

Fig 8. Electromagnetic Compatibility (EMC)

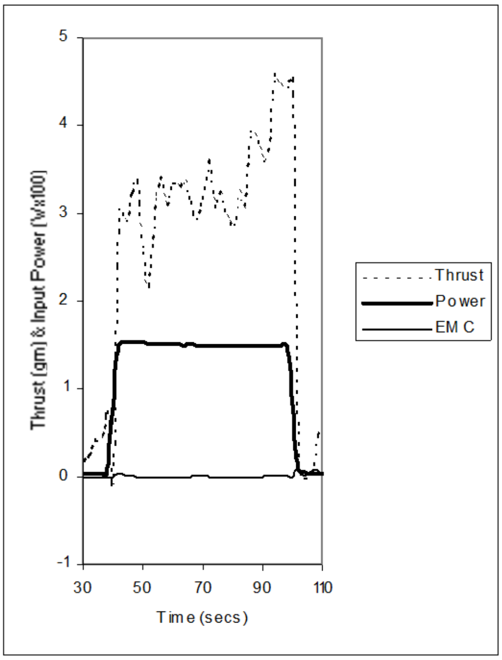

Fig 8 shows the results for a later, higher Q, test run, with the engine on the balance and then with it suspended above the balance. This illustrates the thrust measurements were not subject to EMC effects. Specific thrust for this test was 214mN/kW.

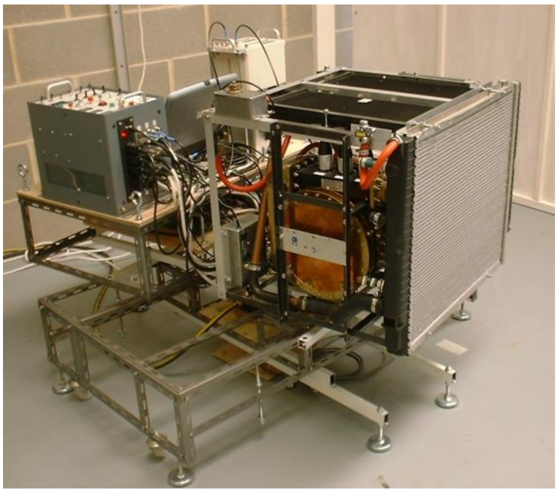

Fig 9. Demonstrator Engine on Dynamic Test

The engine was then mounted on a dynamic test rig enabling it to be "flown" on a rotary air bearing, as shown in fig 9.
The tests simulated the engine moving a 100Kg spacecraft in weightless conditions.

The test programme included acceleration and deceleration runs in both directions, and confirmed the thrust levels measured in the static tests.

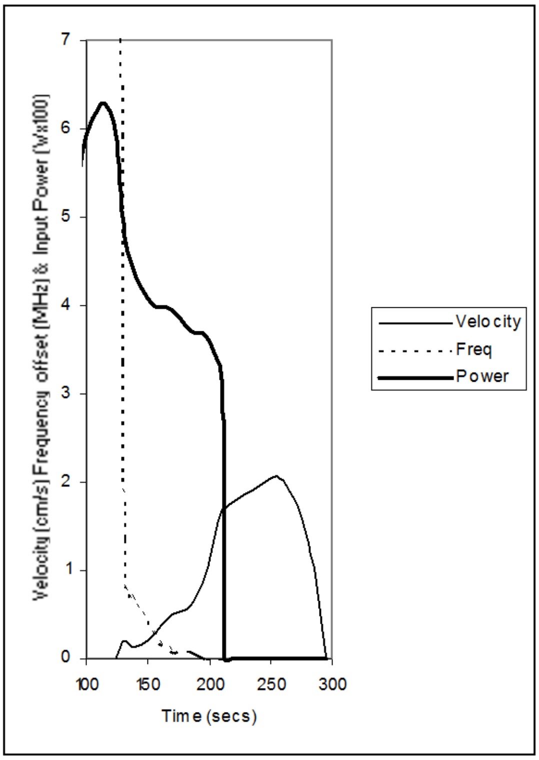

Fig 10. Dynamic test results

Fig 10 gives the result of a typical test run, where the Demonstrator Engine produced a thrust of 10.4 gm against a calibrated friction torque of 7.1 gm. Input power was 421W, giving a specific thrust of 243 mN/kW.

The frequency offset curve shows that initial magnetron thermal drift ends with frequency lock. At this point, 130 secs into the test run, the velocity data shows the start of acceleration under power. The prior thermal drift period, with no acceleration, shows that the thrust is not a result of spurious thermal effects. When the power is turned off, at 210 secs, there is a coast period as the slosh effects of 5kg of coolant maintain a reduced acceleration. This is followed by the deceleration due to the friction torque. A maximum velocity of 2cm/s was achieved and a total distance of 185cm was "flown".

The direction of acceleration was opposite to the direction of thrust, thus conclusively proving that the engine obeys Newton's laws, and that although no reaction mass is ejected, the engine is not a reactionless machine. An electrical reaction occurs between the EM wave and the reflector surfaces of the resonator, resulting in an input impedance change with acceleration. This is seen in the power curve in fig 10.

6. FLIGHT THRUSTER PROGRAMME

The Flight thruster programme covers the design and development of a 300 Watt C Band flight thruster. This has a specified thrust of 85 mN, and a mass of 2.92Kg. Overall dimensions are 265mm diameter at the baseplate and a height of 164mm.

Fig 11 Flight Thruster

The Engineering Model of the Flight Thruster is shown in fig 11. Development testing of the unit, up to a power of 600 W, is under way, and to date, has given a mean specific thrust of 330 mN/kW. This gives a high level of confidence that the specified performance will be achieved on the Flight Model. A major part of the work is in the development of the frequency tracking algorithm. This is needed to ensure the input frequency matches the resonant frequency of the high Q (60,000) cavity, over the full input power range and the qualification temperature specification.

The thruster is designed to be powered from existing flight qualified TWTAs, which are driven from a dual redundant frequency generator unit (FGU) The FGU includes a frequency control loop using feedback signals from the thruster, as shown in the functional block diagram of the complete Flight Engine Fig 12.

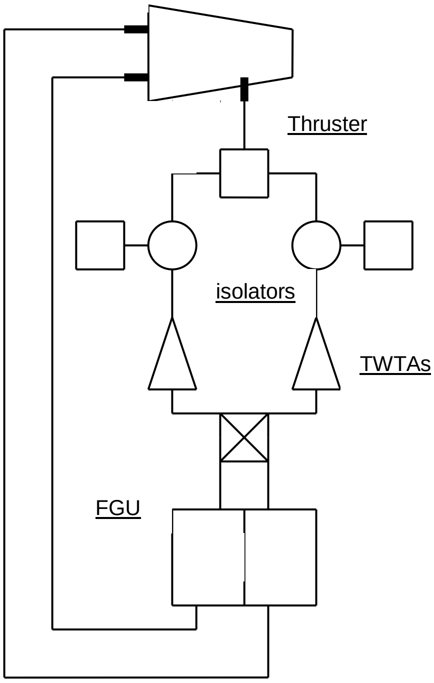

Fig 12. Flight Engine Block Diagram

7. SATELLITE APPLICATIONS

The main applications for flight thrusters will be in-orbit propulsion for Earth orbiting satellites. These will fall into the 3 categories of commercial, military and scientific missions.

There is a major commercial advantage in using EmDrive to transfer large communications and broadcast satellites from an initial LEO to GEO. Studies have shown that the initial launch mass can be halved, with transfer times of less than 40 days, (reference 3). Operational lifetimes can also be doubled.

A clear military requirement can be foreseen, once the technology becomes widely available. Any country capable of orbiting a small satellite to LEO can use EmDrive to covertly manoeuvre the small satellite alongside a major military space asset, in any orbit. Note that EmDrive has no discernable plume signature. It is therefore necessary for future military satellites to have the continuous manoeuvring capability, provided by EmDrive, to counter any such new threat.

Earth orbiting science missions will benefit from EmDrive, in providing continuous drag compensation, allowing lower orbits to be maintained. However the main advantages to science missions will become apparent when EmDrive is applied to long duration deep space missions. Compared to current ion engine performance, studies have shown that EmDrive can decrease spacecraft mass by a factor of 10, increase thrust by a factor of 3, increase thrust period by a factor of 30, whilst maintaining the same input power requirement, (reference 3).

Using the existing flight model design as the starting point, two lines of development will be followed.

Thrust Vector control.

A single plane, 360 degree, pointing mechanism will be developed and qualified to enable a set of four FM thrusters, each mounted on a mechanism, one on each spacecraft side panel, to carry out full 3 axis AOCS functions with the required redundancy. As there are no plume restrictions, the mechanism can be mounted inside the spacecraft, thus easing the environment specification. With each thruster orientated along the same axis, primary propulsion for orbit changing of medium sized satellites is available.

High Power operation.

By mounting the thruster externally on the spacecraft, on the lower panel where the ABM is normally mounted, a set of high power thrusters can provide the primary propulsion for LEO to GEO transfer of large satellites. A high power rating of 3.5kW per thruster can be achieved by up-rating the design, together with the addition of radiating fins. This would produce a target static thrust of 1N per thruster.

8. SUPERCONDUCTING DEMONSTRATOR PROGRAMME

The first phase of this programme was an experimental superconducting thruster. This low power, HTS device operates at liquid nitrogen temperature, and is designed for very high Q and consequently high specific thrust.

Fig 13 Experimental Superconducting Thruster

Fig 13 shows the thruster, which operates at 3.8 GHz, and was designed using an update of the software used for the previous S band designs. Super-conducting surfaces are formed from YBCO thin films on sapphire substrates.

Small signal testing at 77 deg K confirmed the design, with a Q of 6.8×10^6 being measured.

This measured Q is the highest value (by a factor of 10) that has been reported for any HTS cavity. The work formed the basis of a separate design study for a small 500 kg Demonstrator Vehicle, leading to the design of a 315 Tonne Hybrid Spaceplane, which offers a truly disruptive operational capability, (reference 4).

REFERENCES

1. MAXWELL J.C. ‘A Treatise on Electricity and Magnetism’
1st Edition (Oxford University Press 1873) p.391.

2. CULLEN A.L. ‘Absolute Power Measurements at Microwave Frequencies’ IEE Proceedings Vol 99 Part IV 1952 P.100

3. SHAWYER R.J. ‘ The Development of a Microwave Engine for Spacecraft Propulsion’
JBIS Vol. 58 Suppl.1, 2005.

4. SHAWYER R.J. ‘The EmDrive Programme – Implications for the Future of the Aerospace Industry’
CEAS 2009 proceedings. Session 11. Oct 2009